PERFORMANCE IMPROVEMENT OF THE R744 TWO-PHASE EJECTOR WITH AN IMPLEMENTED SUCTION NOZZLE BYPASS

Jakub Bodys [(a)], Jacek Smolka [(a)], Krzysztof Banasiak [(b)], Michal Palacz [(a)], Michal Haida [(a)], Andrzej J. Nowak [(a)]

[(a)] Institute of Thermal Technology (ITT), Silesian University of Technology (SUT), Gliwice, 44-100, Poland, jakub.bodys@polsl.pl
[(b)] SINTEF Energy Research, Trondheim, 7465, Norway, krzysztof.banasiak@sintef.no

Abstract
In this study, the concept of an R744 ejector with a bypass duct of a suction nozzle was presented. The design of the geometry and bypass positioning in a mixing section, and the idea of regulation, as well as integration, with a suction nozzle duct was described. A preliminary numerical analysis of the proposed bypass geometry was also presented. The computational platform *ejectorPL* integrated with an extensively validated mathematical model of transcritical R744 two-phase flow was used. Motive nozzle inlet and suction nozzle inlet conditions reflecting gas cooler and evaporator conditions characteristic of large systems, such as supermarket refrigeration units, were examined. Three different separation pressures in liquid receivers were assumed for two bypass geometries and six bypass inlet positions. The bypass positioning as a function of a mixer length was presented. Uniquely positive results were obtained for the lowest pressure conditions. Namely, the increment of the suction mass flow rate was substantial and equal to 36.9% for the bypass angle of 19°. Hence, the bypass implementation resulted in distinct potential of an efficiency improvement - from 22.2% to 30.4%. A higher pressure lift case did not result in any improvement of the ejector work. The influence of the bypass geometry on the overall ejector efficiency was preliminarily characterised. Finally, the pressure distribution in the bypass type ejector was described.

Keywords
R744, carbon dioxide, transcritical ejector, two-phase ejector, bypass ejector, efficiency improvement

Nomenclature

Acronyms and abbreviations

CFD	Computational Fluid Dynamics
COP	Coefficient of Performance
GWP	Global Warming Potential
HEM	Homogeneous Equilibrium Model
HF	Hydrogen fluoride
HFC	Hydrofluorocarbons R744 Carbon dioxide
HVAC	Heating Ventilation and Air Conditioning
IHX	Internal Heat Exchanger
MER	Mass Entrainment Ratio
MN	Motive nozzle
OC	Operating Conditions
R134a	Tetra-fluoro-ethane
SN	Suction nozzle
TFA	Tri-fluor-oacetic acids

Roman Letters

c	specific heat, J kg^{-1} K^{-1}
d	width, m
E	total enthalpy, J kg^{-1}
h	specific enthalpy, J kg^{-1}
k	effective thermal conductivity, W m^{-1} K^{-1}
L	length, m
$\dot{m}$	mass flow rate, kg s^{-1}
p	pressure, Pa

This is a post-print version of an article published in International Journal of Refrigeration
DOI: 10.1016/j.ijrefrig.2018.03.020

r	radius, m
s	specific entropy, J kg^{-1} K^{-1}
t	time, s
T	temperature, K
U	velocity vector, m s^{-1}

Greek Letters

β	angle, °
η	overall ejector efficiency, %
χ	Mass Entrainment Ratio, -
μ	dynamic viscosity, J kg^{-1}
ρ	density, kg m^{-3}
τ	stress tensor, N m^{-2}

Subscripts

BPS	bypass
BSC	bypass suction chamber
in	ejector inlet
is	isentropic
l	liquid phase
MIX	mixer
out	ejector outlet
p	constant pressure
v	vapour phase

1. Introduction

Global phase-in of environmentally friendly working fluids has had a crucial impact on the refrigeration area. According to the so called F-gas regulation, the vast majority of present refrigeration units working with synthetic refrigerants should be improved or totally replaced before 2022 (European Commission, 2014). Legal regulations related to requirements for working fluids in a mobile air conditioning unit have already banned tetrafluoroethane (R134a) in cars produced in 2017 (European Commission, 2006). In this situation, re-introduction in the commercial applications of carbon dioxide (R744) should be considered as one of the most promising working fluids. The obligatory phase-in of environmentally friendly refrigerants in the automobile market and already proposed applications for heating ventilation and air conditioning (HVAC) in trains additionally proves the safe exploitation of these systems (European Commission, 2006; Hafner, 2016).

According to non-flammability and non-toxicity of carbon dioxide, the highest safety level of exploitation is ensured in such installations (American Society of Heating Refrigerating and Air-Conditioning Engineers, 2016). Finally, R744 gives a reference level for a global warming potential (GWP) factor, while it takes the value of 1. No depletion of the ozone layer is another advantage of carbon dioxide, but this advantage also applies to a whole group of natural refrigerants. Due to the local and global exploitation of safety mentioned, both matters should be satisfied simultaneously. Meanwhile, newly produced synthetic refrigerants characterised by a very low GWP factor might be environmentally friendly working fluids, but they have serious disadvantages. Namely, refrigerants from the R1234 group are characterised by safety class A2/L (American Society of Heating Refrigerating and Air-Conditioning Engineers, 2016), where the possibility of safe service and maintenance have been confirmed (Imamura and Kamiya, 2015). However, the burning process results in toxic products such as trifluoroacetic acid (TFA) or hydrogen fluoride (HF) with a real danger to human health in closed spaces such as garages (Hurley et al. 2008).

According to the thermodynamic characteristics of carbon dioxide, in addition to the environmental and safety advantages mentioned, some features bring the benefits of an actual R744 refrigeration and heating system efficiency. According to pressure levels of the high and low pressure side, in the case of R744, the pressure ratio is significantly lower than in the case of other common working fluids. As a consequence, a higher isentropic efficiency of the

This is a post-print version of an article published in International Journal of Refrigeration
DOI: 10.1016/j.ijrefrig.2018.03.020

standard piston compressors is provided (Joneydi et al. 2016). In the case of component sizing, the carbon dioxide system dispenses a higher volumetric refrigeration/heat capacity than common hydrofluorocarbons (HFCs). Consequently, smaller components such as heat exchangers and compressors could be utilised in CO_2 units, resulting in overall compact sizing of such an installation. However, the CO_2 cycle results in significant losses during a throttling process that starts from an area close to the critical point (Lorentzen, 1994). The necessity of operation in this region is a consequence of a relatively low critical point for R744 of approximately 31.06°C (IPU & Department of Mechanical Engineering of Technical University of Denmark, 2017). Moreover, these losses cause the performance of the system to deteriorate to a level that is lower than the appropriate systems with synthetic fluids (Lorentzen, 1995). Hence, a design process should ensure as high as possible of an amount of heat sinks, i.e., an integration with heating processes, to reduce the temperature of the fluid before the throttling process (Farsi et al. 2014; Ge et al. 2015). One of the most promising heat receivers is the production of hot tap water or even district heating (Byrne et. al 2009; Minetto et al. 2016). First examples such as office buildings and housing estates proved the reliability and cost effective exploitation of heating and cooling integration (Ignacio et al. 2017; Minetto et al. 2016).

Another large possibility for cycle improvement is the recovery of a relatively high potential of work related to the throttling process of carbon dioxide in comparison to synthetic refrigerants (Lorentzen, 1994). Ejectors are the most likely solution for an indirect work recovery in refrigeration units (Elbel & Lawrence, 2016). The reasons are related to reliability, no moving parts, relatively simple construction in comparison to direct expanders, e.g., a gear expander. Moreover, the ejector functionality allows for additional fluid circulation or operation as a pumping device (Haida et al. 2016; Lawrence & Elbel, 2015).

According to the efficiency improvement possibilities mentioned as well as the growing functionality of the carbon dioxide systems equipped in ejectors, a wide range of studies focused on a refrigeration cycle with this method of work recovery was provided in the literature. One of the first studies focused on the ejector application for the refrigeration cycle improvement was performed by Elbel and Hrnjak (2008). This study concerned various operating conditions for the R744 ejector refrigeration system with an internal heat exchanger (IHX). According to this experimental research, the system coefficient of performance (COP) was improved by 8% in comparison to a traditional system based on the throttling valve. Nevertheless, the reported ejector efficiency was below 20%; hence, the results of this study would show even better perspective for such a system after improvement of the work recovery efficiency. Next, an experimental comparison by Lucas and Koehler, showed a COP improvement of 17% due to the ejector implementation (Lucas & Koehler, 2012). The authors investigated the influence of the high-pressure side on the ejector performance and overall performance of the system under a wide range of operating conditions. In addition to the COP improvement mentioned previously, good possibilities of R744 transcritical system operation under relatively high ambient conditions were predicted. More advanced solutions for large power CO_2 ejector refrigeration systems such as those used in supermarkets were proposed by Hafner (Hafner et al. 2014). A state-of-the-art R744 installation equipped in parallel working ejectors that composed a multi-ejector block provides the wide perspective for operating conditions at high temperature heat rejection. The authors investigated three European sub-climates where mathematical simulations note that a reference system COP could be improved up to 20% under high ambient conditions and even up to 30% under winter conditions. In the study of Haida (Haida et al. 2016), the solution proposed by Hafner (Hafner et al. 2014) was experimentally investigated to compare the multi-ejector system with the previous generation of a parallel compression system. The global evaluation of both systems results in a COP

This is a post-print version of an article published in International Journal of Refrigeration
DOI: 10.1016/j.ijrefrig.2018.03.020

improvement at the level of 7% and exergy efficiency improvement of up to 13% in the case of the system supported by the multi-ejector pack.

Regarding ejectors as the most promising application for COP improvement, many authors provided studies concerning the performance of this device. An experimental approach based on the direct system COP improvement, as well as numerous studies focused on the most efficient ejector performance, have been provided in the literature. In the experimental study provided by (Masafumi et al. 2009), a variant analysis of a convergent-divergent motive nozzle for an R744 ejector operating at various suction pressures was presented. The experimental results were additionally compared with Isentropic Homogeneous Equilibrium Theory to obtain a range of applicability for such calculations.

The next experimental study presented by (Nakagawa et al. 2011) concerned the influence of an ejector mixing length on a R744 refrigeration cycle with an IHX. According to the reported results, COP improvement up to 26% is possible when proper mixing length is ensured. Finally, the relationship between the mixing section and each of the crucial evaluation parameters such as the ejector efficiency, entrainment ratio, pressure lift and system COP was discussed.

In contrast to experimental analysis, a wider range of geometrical parameters could be analysed based on numerical models. Comprehensive review of mathematical models developed for carbon dioxide flow in ejectors was provided in the work of (Nowak et al. 2015). These authors analysed the development path of the flow models starting from the basic 1-D approach to advanced computational fluid dynamics (CFD) simulations. The 1-D approach mentioned was used by (Liu et al. 2012). Relatively simple 1-D simulations were used for evaluation of the influence of the ejector geometry on overall ejector performance. The authors investigated two different lengths of a pre-mixing chamber showing better performance of the shorter chamber. Moreover, the ratio between the diameter of a mixing section and the ejector throat diameter were analysed, indicating a very sensitive and non-linear relationship of these parameters.

A more advanced approach based on the CFD was used by (Banasiak et al. 2014). That work described the influence of the mixer geometry parameters on local and global ejector performance. The computational tool was validated based on a wide range of experimental operating conditions characteristic of supermarket applications. Irreversibility analysis of each ejector section confirmed the crucial influence of the mixing section in each of three flow patterns investigated. A similar approach enhanced with the entropy generation simulation was used by (Sierra-Pallares et al. 2016). These authors utilised a transport equation to obtain a local value of the entropy generation in three different geometries of an ejector mixing section. The results showed domination of a fluctuating viscous dissipation as a source of the entropy generated.

According to the substantial developments of R744 ejectors, one of the most advanced numerical analysis investigations was delivered by (Palacz et al. 2017), where full optimisation of ejector geometrical parameters was provided. A validated computational tool was used to simulate a transonic two-phase flow of the carbon dioxide trough ejector characteristic of the high pressure supermarket conditions (Palacz et al. 2015; Smolka et al. 2013). Six parameters describing the ejector shape were taken into the objective function of the optimisation procedure. The trends obtained were similar for each of four ejector sizes and denote an approximately 6% efficiency improvement to the already highly efficient (30%) ejectors. A longer mixing section and increased angle of a motive nozzle diverging section were proposed to improve the ejector performance.

According to the numerous studies presented, well developed geometrical relationships of an ejector construction allowed for design of high efficiency ejectors under the given pressure conditions. A further development step was focused on ensuring the proper regulation idea according to the variable load of a refrigeration unit. Two different approaches were proposed in the literature. First, a solution based on an adjustable geometry ejector was experimentally

This is a post-print version of an article published in International Journal of Refrigeration
DOI: 10.1016/j.ijrefrig.2018.03.020

examined by (Liu et al. 2012). Authors presented satisfactory results for controlling cycle performance based on needle insertion into the ejector throat. The COP improvement up to 60% was reported due to regulation based on the controllable ejector with a needle. Nevertheless, in this study, an air conditioning cycle was used for the experimental tests with a relatively low compressor power of approximately 10 kW.

Evaluation of a controllable ejector performance for various loads characteristic of large refrigeration units such as in supermarkets was presented by (Smolka et al. 2016). A full numerical comparison of a controllable and fixed geometric efficiency was based on the same baseline models characterised by high efficiency as in the work of (Palacz et al. 2017). The results noted a very sensitive function of the ejector efficiency relative to a needle position. In the case of a needle position that is too deep, the suction flow was totally choked. Nevertheless, proper adjustment of the needle position resulted in increased ejector efficiency of up to 25% in comparison with the fixed ejector geometry (without the needle).

A second solution is characterised by the idea of regulation opposite from the first described controllable ejectors. Namely, a solution based on several parallel working ejectors and binary regulation of such a system was proposed by (Hafner et al. 2014). Due to discrete regulation possibilities, a linear profile for controlling this device is ensured. Experimental performance mapping of this multi-ejector module was done by (Banasiak et al. 2015). The reported overall performance of ejectors contained in the multi-ejector module was on the level of 30%. The power of the laboratory facility used was 70 kW with a temperature of 35°C at a gas cooler outlet where the evaporation temperature was -3°C to mimic supermarket operation in a warm south European climate. Those authors examined a wide range of operating conditions and confirmed applicability of this device to cooperation with a classical high pressure throttling valve.

The multi-ejector module mentioned in the previous paragraph was evaluated numerically in the work of (Bodys et al. 2017). The parallel work of the ejectors examined including motive, suction and outlet collectors was based on the 3-D simulations. The Homogeneous Equilibrium Model of transonic two-phase R744 flow was developed by (Smolka et al. 2013) and introduced to the computational tool *ejectorPL* (available online: www.itc.netrom.pl) described by (Palacz et al. 2015). The operating conditions tested were characteristic of the high ambient conditions in a southern European climate. The numerical evaluation confirmed the possibilities of linear adjustment to the system load. Nevertheless, the overall efficiency of the multi-ejector pack was decreasing with increasing load. The authors stated that these increasing losses are related mainly to the mixing processes in the outlet collector. The benefits offered by full 3-D domain simulation allowed the independent analysis of each ejector in the case of the parallel work mode. This analysis resulted in the stable work of each device with a high efficiency of approximately 35%. Finally, some propositions for further improvement were stated in the optimisation of the outlet collector.

The regulation methods mentioned provide the possibility of the load regulation. Nevertheless, as described in (Banasiak et al. 2014; Liu et al. 2012; Nakagawa et al. 2011; Nakagawa et al. 2009; Palacz et al. 2017; Smolka et al. 2013, 2016), the high sensitivity of ejectors to operating conditions and designed geometrical parameters forces these devices to work with an optimal efficiency that is close to on-design operating conditions. Moreover, the optimal efficiency could be obtained only with a specified mass entrainment ratio and a corresponding pressure lift. However, according to various systems operations, an ejector is forced to work at a variable pressure lift. Then, the efficiency decreases due to a decreasing entrainment ratio based on unfavourable pressure distribution along the ejector axis and consequently, reduced suction phenomena.

To ensure a suspension of such a situation, an additional duct called bypass could take the role of a suction nozzle substitute. The duct mentioned, located in the ejector diffuser, would provide

This is a post-print version of an article published in International Journal of Refrigeration
DOI: 10.1016/j.ijrefrig.2018.03.020

a bypass flow to the suction nozzle. Simultaneously, the suction stream would be delivered in a more favourable pressure region. The idea of the bypass duct was proposed by the authors of (Chen et al. 2016b) and examined by (Chen et al. 2016a). The analysis contained three different pressure lifts between the suction and the outlet ports. The results were reported after some geometrical optimisation of the bypass duct in the second of the papers mentioned (Chen et al., 2016a). Namely, in the lower pressure case examined, the improvement of the mass entrainment ratio was enlarged from 10.7% (baseline design (Chen et al. 2016b)) to 32.8% due to the optimised position of the bypass. Moreover, after some corrections of the bypass shape, the reported improvement was 48.7%. Nevertheless, this large improvement was examined for the narrow range of operating conditions. Next, analysis of the bypass positions and its shape was quite limited, concerning only simple orthogonal duct shapes. In addition, the authors of that study used air as a working fluid, and the ideal gas law was used for the density calculations. Moreover, the pressure at the suction port and the bypass duct was assumed to be constant. Finally, the suction nozzle and the bypass duct were simulated as separate ejector ports; an analysis of the suction nozzle and the bypass integration was not conducted. However, it could be stated that, further studies of this ejector concept might deliver some prospective results.

In this study, the bypass-type ejector is proposed and analysed for CO_2 applications. To the best of the knowledge of the authors, the bypass investigation in R744 ejectors for refrigeration applications has not been provided to date. The bypass geometry and its positioning, the idea of regulation, as well as the integration with the suction nozzle duct, were proposed and discussed. Adapting the previously developed (Smolka et al. 2013) and well validated mathematical model of transcritical R744 two-phase flow (Palacz et al. 2015; Smolka et al. 2013), the analysis of the bypass concept was performed. The series of variant numerical simulations was provided using the computational platform *ejectorPL* (Palacz et al. 2015). The motive nozzle and suction nozzle inlet conditions reflecting typical gas cooler and evaporator conditions for large systems such as supermarket refrigeration units were examined for three different levels of the ejector outlet pressure (corresponding to pressures in the liquid receiver). Promising results of the mass entrainment ratio were obtained for the lowest pressure conditions leading to the same efficiency as in the case of the ejector operation with higher separation pressures. In addition, the distribution of the sucked stream between the suction nozzle and the bypass duct were analysed in an axisymmetric CFD study. The pressure and Mach number distributions along the ejector axis as well as in the bypass location were presented and discussed. Finally, potential shape optimisation for higher evaporation pressures was also given.

2. Bypass ejector idea

Ejector operation with pressure lift decreased beyond the rated (design) conditions typically results in lower overall efficiency of the ejector. Physical reasons are based on the unfavourable pressure distribution in a mixing zone due to chocked flow conditions in this area. To overcome geometrical constraints and increase the suction flow rate, an additional duct introduced after the blocked flow region might be considered. This duct plays the role of the suction nozzle bypass, and this nomenclature will be used in this study. The proposed solution for carbon dioxide cycles could have a great impact on the overall COP of the system. Moreover, according to the proposed regulation idea presented in Fig. 1, no additional connector will be required. Implementation of bypass is based on a classic ejector geometry. Hence, basic ejector sections such as converging-diverging motive nozzle, suction nozzle, mixer and diffuser are indicated in Fig. 1, where one half of an ejector geometry with respect to the device axis is schematically presented. The bypass duct volume was marked by a blue area located in the suction duct before the suction nozzle. The shape and position of the suction nozzle duct are crucial for effective bypass implementation. Simultaneous connection of the suction nozzle and bypass with only one inlet suction port (see Fig. 1) gives more reliability and allows for avoidance of an

This is a post-print version of an article published in International Journal of Refrigeration
DOI: 10.1016/j.ijrefrig.2018.03.020

additional valve. In this paper, the concept of the bypass opening is based on two separate parts of the ejector. The two parts mentioned are obtained as a result of the precise cutting of the standard ejector. Therefore, part A and part B will be created. Part A is stationary. The volume of the bypass duct (blue in Fig. 1) is obtained after offset of the moving part B in the direction of the ejector outlet. A proper location of the suction port allows for supplying both suction nozzle and bypass. Dependent on displacement of part B, proper bypass width is obtained. In the case of the zero offset, part A and B are connected, and the standard fixed ejector geometry is utilised.
The proposed solution does not require any additional pipeline systems for the bypass activation, apart from a system enabling retraction of part B from the rest of the ejector geometry.

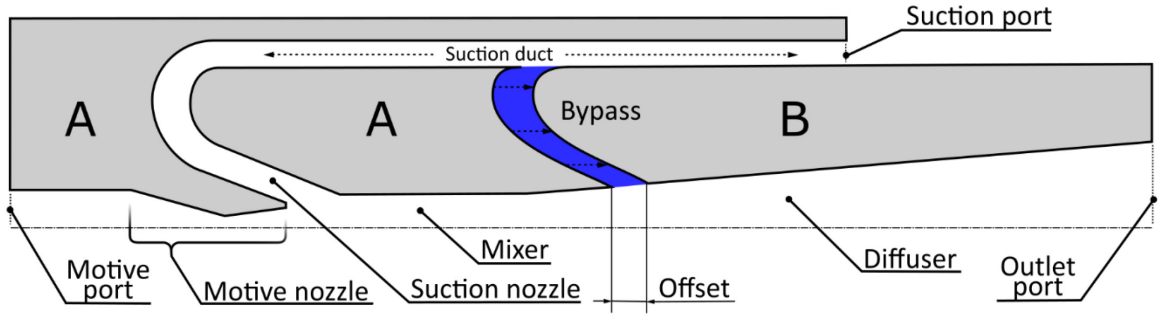

Figure 1. Idea of bypass implementation to the fixed-geometry ejector.

In this study, the proposed bypass idea was preliminarily investigated using CFD methods. Hence, the main efforts were focused on the flow analysis and potential of overall improvement in the selected operating conditions. The design development of the bypass ejector should be considered as the other study involving additional factors, i.e., the manufacturing of a regulation mechanism and its sealing, as well as the connection between the outer and inner part A. Such a study should be preceded by predictions of the available potential of the bypass solution. The data mentioned are included in this paper.
The solution presented in the paper was examined with the approach based on the axis-symmetry domain in order to evaluate main assumptions of the proposed bypass idea. Namely, analysis of the bypass duct performance in the case of a transcritical R744 ejector and the idea of the moving parts (part A and part B) are not dependent on the domain dimensionality. It is due to that the domain boundaries were limited at the diffuser outlet. Hence, any regulation mechanism introduced to the flow domain after the diffuser part in order to move part B and unlock the bypass duct would not affect carbon dioxide flow in the mixing section and, in consequence, the performance of the ejector. In addition, the modifications related to the bypass idea proposed in the paper are definitely possible to be designed and then produced.

3. Computational procedure and simulation range

3.1. Ejector geometry without bypass

Simulations of the presented bypass-type ejector were performed on the basis of one of the standard ejector geometries that was used in the previous studies (Bodys et al. 2016; Haida et al. 2016; Palacz et al. 2015; Smolka et al. 2013, 2016). This geometry is presented in Fig. 2. The diverging-converging motive nozzle is described by two angles of 12° and 2°, and the diameters of the inlet duct are at 3.8 mm with the outlet at 1.6 mm. Moreover, the dimensions of the pre-mixing chamber are given in a form of the converging angle of 38° and the length of 3.7 mm. The diffuser angle is 5°. Considering the main goal of this analysis, namely, checking of the bypass idea performance, the mixing chamber and diffuser length are defined in the

This is a post-print version of an article published in International Journal of Refrigeration
DOI: 10.1016/j.ijrefrig.2018.03.020

dimensionless universal form. Thus, the proper relationship of the bypass geometry is presented in Fig. 3.

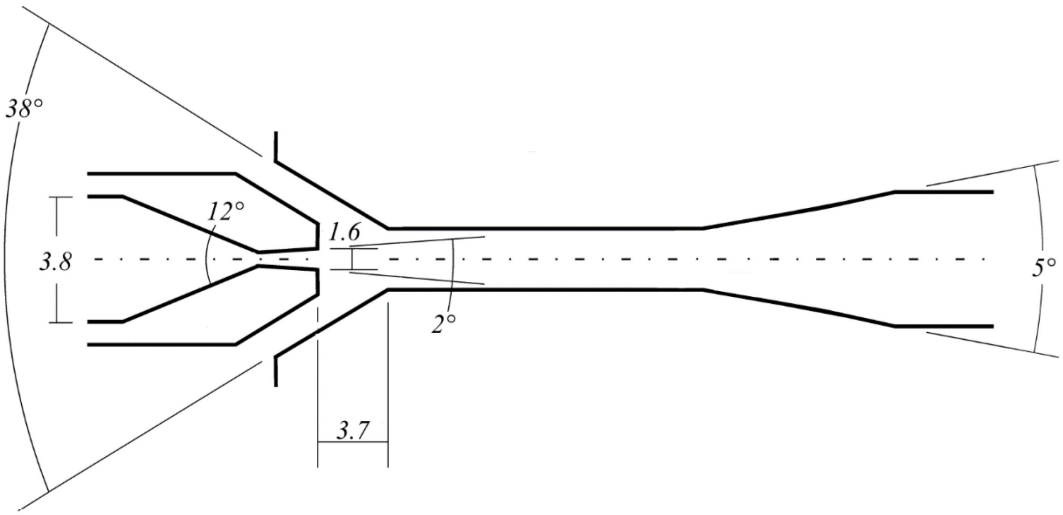

Figure 2. Geometry of baseline ejector used in this study (dimensions given in *mm*).

3.2. Ejector geometry with bypass

The shape of the bypass was obtained on the basis of the suction nozzle modification and generation of a proper turn, selecting two radii (r_1, r_2) and the dimension L_1. Next, the bypass entered the diffuser volume with the angle β between the ejector axis and walls of the bypass. Moreover, the dimension d_1 was a width of the bypass. In the simulations performed, the assumption of a bypass width equal to half of the mixer diameter was used.

The parameters used for definition of the bypass positioning are L_{MIX} and L_{BPS}. The dimension L_{MIX} describes the length of the ejector mixer. The second dimension, i.e., introduced as L_{BPS}, gives the position of the connection of the bypass and the diffuser wall.

For a complete description of the bypass geometry, dimension L_{BSC} was also introduced. This dimension denotes the length of the bypass suction chamber and varies according to the angle β and the bypass position. This dimension will also be used to discuss the results obtained. The beginning of the bypass suction chamber is defined by the point located closer to the mixing chamber (i.e., L_{BPS} - L_{BSC}), while the end of the bypass suction chamber is defined as the point closer to the ejector outlet (i.e., L_{BPS}). The bypass described should obviously be linked with the geometry of the fixed-geometry ejector presented in Fig. 2.

This is a post-print version of an article published in International Journal of Refrigeration
DOI: 10.1016/j.ijrefrig.2018.03.020

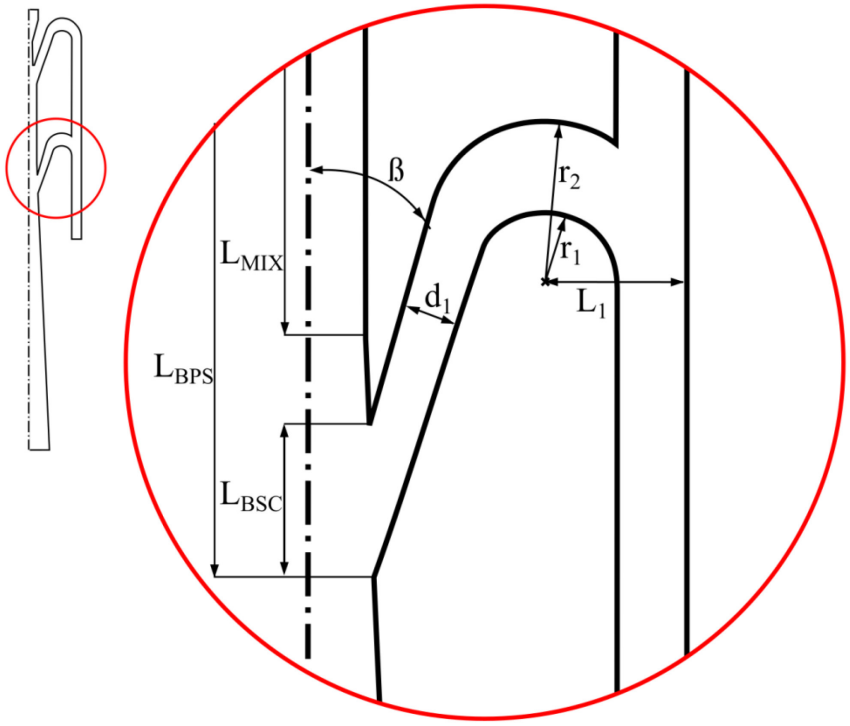

Figure 3. The proposed bypass geometry.

Finally, the bypass position is presented in the form of dimensionless ratio between L_{BPS} and L_{MIX}:

$$Position = \frac{L_{BPS}}{L_{MIX}} \quad (1)$$

This parameter shows how far the bypass is located inside the diffuser. The bypass idea was tested in its several positions. Moreover, two angles β were examined during the computational procedure, i.e., 19° and 38°. The angle of 19° was assumed as a direct translation of the suction nozzle angle, while the second angle was a factor of two larger than the first angle. Because of some geometrical restrictions on the bypass suction chamber, the positions examined were not the same for each angle.

The bypass configurations considered are schematically presented in Table 1. In the sketch of the baseline ejector, the dotted red frame marks an area where the bypass was introduced. Moreover, the dotted green line shows the position where the mixer chamber meets with the diffuser section. This dotted green line presented in the next rows of Table 1 helps to show differences between particular positions of the analysed bypasses and their connection with the mixer and diffuser sections. Generally, four bypass domains for each angle were generated. According to the bypass position defined in Eq. (1) and the geometry dimensions presented in Fig. 3, Position 1.0 denotes that the whole length L_{BSC} is found in the mixer area. Positioning in the mixer and diffuser connection was avoided to maintain the length of the mixing section (used in the position definition in Eq. (1)) characterised by a constant diameter. Next, positions were selected in such a way that the bypass suction chamber began exactly in the baseline diffuser that resulted in Position 1.2 of 38° and Position 1.29 of 19° (described as Position 1.3). In a series of 38°, the distance of 0.2 mixer length was added to Position 1.2, resulting in Positions 1.4 and 1.6 of the bypass with larger angle. In the case of a smaller angle, the length of the bypass suction chamber is larger than in the case of 38°. Hence, only 0.1 mixer length was added, resulting in Positions 1.39 and 1.49 and described as 1.4 and 1.5, respectively.

This is a post-print version of an article published in International Journal of Refrigeration
DOI: 10.1016/j.ijrefrig.2018.03.020

Finally, Position 1.59 for the smaller angle was not considered, according to an analysis of unsatisfactory results obtained for previous positions. Altogether, six different bypass positions were analysed for both mentioned angles based on the numerical simulations.

Table 1. Geometries considered in simulations of the bypass idea.

Position	Bypass angle β	
	38°	19°
Baseline	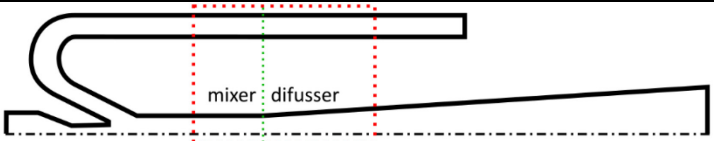	
1.0	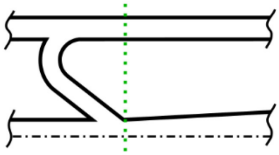	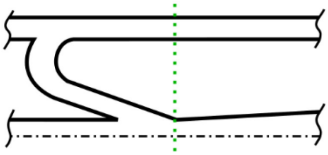
1.2		
1.3		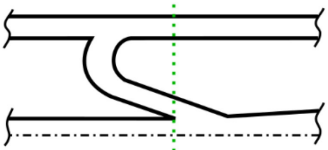
1.4	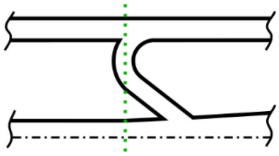	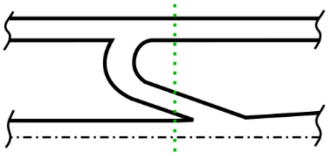
1.5		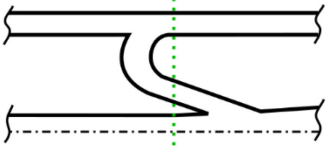
1.6	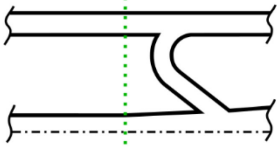	

3.3. Mathematical model

In this paper, the mathematical model presented and validated by (Smolka et al. 2013) was used for all simulations. Namely, CO_2 two-phase transonic flow through an ejector was computed using the Homogeneous Equilibrium Model (HEM) with turbulence modelling ensured by the realisable *k-ε* model. In the work of (Palacz et al. 2015), this formulation was extensively tested using a number of ejector geometries and operating conditions for the carbon dioxide flow. Due to the modified numerical domain of the ejector (bypass duct), a verification of the turbulence model needs to be performed. However, until relevant data based on the experimental tests focused on the local flow field visualisation will be available such a verification process is not possible. Nevertheless, the employed approach of the turbulence modelling was successfully validated in the study of R744 ejector optimisation (Palacz et al. 2017) and multi-ejector block simulations (Bodys et al. 2017). For this reason, the realisable *k-ε* model was utilised in this

This is a post-print version of an article published in International Journal of Refrigeration
DOI: 10.1016/j.ijrefrig.2018.03.020

study as well. In the HEM model, the thermodynamic and mechanical equilibrium between the liquid and the gaseous phase is assumed. The flow parameters were calculated solving the CFD governing equations, as given by (Anderson, 1995) and (Chung, 2010).

$$\frac{\partial \rho}{\partial t} + \nabla \cdot (\rho \boldsymbol{U}) = 0 \tag{2}$$

where ρ is the density, t is the time, and U is the velocity vector,

$$\frac{\partial (\rho \boldsymbol{U})}{\partial t} + \nabla \cdot (\rho \boldsymbol{U}\boldsymbol{U}) = -\nabla \cdot p + \nabla \cdot \boldsymbol{\tau} \tag{3}$$

where p is pressure and τ is the stress tensor,

$$\frac{\partial (\rho E)}{\partial t} + \nabla \cdot (\rho \boldsymbol{U} E) = \frac{\partial p}{\partial t} + \nabla \cdot (k \nabla T + \tau \cdot \boldsymbol{U}) \tag{4}$$

where E is the total enthalpy, k is the effective thermal conductivity, and T is the temperature. Since only steady state computations were carried out, all time derivatives in Eqs. (2) - (4) have been neglected.

The classical definition of the total enthalpy as a sum of the mixture-specific enthalpy h and the kinetic energy was implemented (Anderson, 1995).

$$E = h + \frac{U^2}{2} \tag{5}$$

An assumption of liquid l and vapour v phase thermodynamic equilibrium is forced via the following additional conditions.

$$\begin{cases} p_l = p_v = p \\ T_l = T_v = T \\ \boldsymbol{U}_l = \boldsymbol{U}_v = \boldsymbol{U} \end{cases} \tag{6}$$

Thus, the HEM approach characterises the modelled fluid properties as a function of the specific enthalpy and pressure based on:

$$\{\rho, \mu, k, c_p\} = f(p, h) \tag{7}$$

where μ is the dynamic viscosity, and c_p is the specific heat capacity. All the properties for carbon dioxide treated as a real fluid were obtained based on REFPROP libraries ver. 9. Such an approach is given by (Lemmon et al. 2010).

Validation of the above model was originally published by (Smolka et al. 2013) for two popular refrigerants. Additionally, a model of the transonic two-phase flow of R744 was validated against experimental data from the SINTEF test rig. The model accuracy was evaluated based on the mass flow rates and was typically within 10–15%.

The extended validation was provided by (Palacz et al. 2015), where a wide range of operating conditions characteristic of the supermarket operating regimes was tested. The results of that work showed the applicability region of the HEM model. Furthermore, the model accuracy decreased for the motive nozzle operating conditions distributed slightly above/near to the saturation line. Considering the model accuracy and limitations, the operating conditions selected for this investigation were within the range of the satisfying HEM accuracy (Palacz et al. 2015).

Moreover, in the work of (Palacz et al. 2015), the model proposed by (Smolka et al. 2013) was implemented to computational platform *ejectorPL* schematically, as presented in Fig. 4. This

This is a post-print version of an article published in International Journal of Refrigeration
DOI: 10.1016/j.ijrefrig.2018.03.020

platform was used for the baseline case and for every examined bypass position. Due to the computational procedure employed, the same number of iterations was needed in every simulated case. Levels of the residuals after the last iteration were below a value of 10^{-6} for all the governing equations. According to the scheme presented in Fig. 4, the post-processing operations were executed in the same manner for all configurations considered.

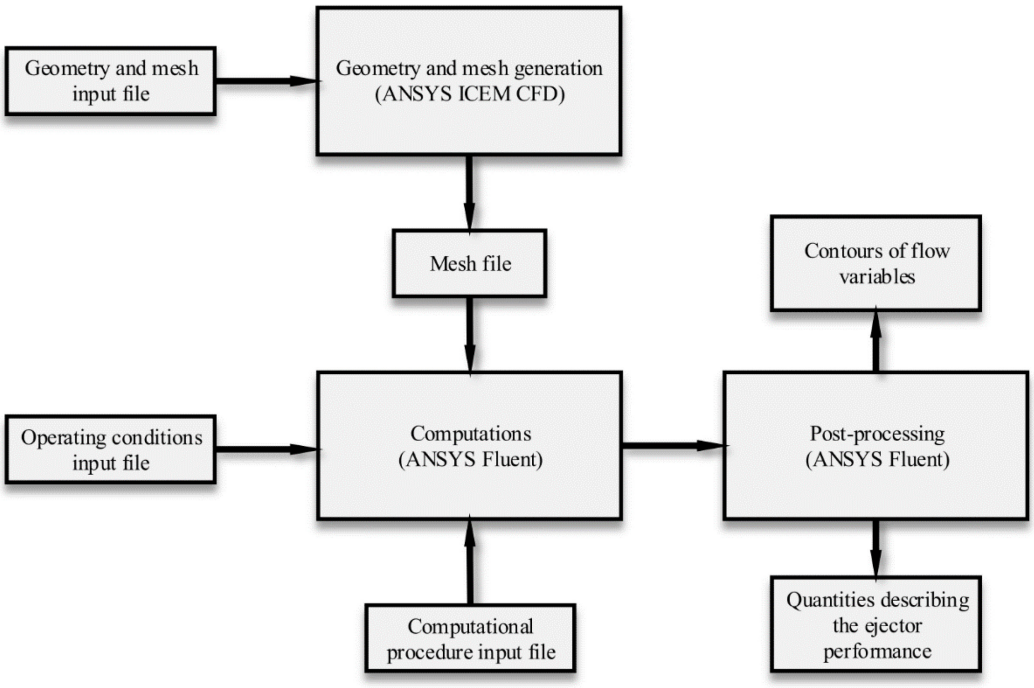

Figure 4. Scheme of computational platform *ejectorPL* (Palacz et al. 2015).

3.4. Operating conditions

Domains generated for various bypass domains were simulated for three groups of operating conditions (OCs). The parameters collected in Table 2 were defined as boundary conditions in the computational procedure. The motive pressure is typical for transcritical operation of a refrigeration unit in a supermarket. The temperature of the motive stream can be related to summer conditions of southern Europe. The evaporation temperatures at the suction nozzle inlet are typical for chilling cabinets. The pressure of the intermediate pressure receiver defined at the ejector outlet was taken as a variable to simulate various pressure lifts of 4 bar, 6.5 bar and 9 bar.

Table 2. Parameters defined as boundary conditions for the simulations performed.

OC No.	Motive nozzle		Suction nozzle		Outlet
-	bar	°C	bar	°C	bar
1					32.0
2	84.5	32.0	28.0	1.0	34.5
3					37.0

3.5. Evaluation of the ejector performance

An evaluation of both configurations was performed using the ejector efficiency definition according to the work of (Elbel & Hrnjak, 2008). This efficiency of the ejector is given as a ratio between a recovered work and maximum available work delivered in the motive nozzle. Namely, the numerator is defined as a difference of enthalpies obtained from an isentropic and

This is a post-print version of an article published in International Journal of Refrigeration
DOI: 10.1016/j.ijrefrig.2018.03.020

isenthalpic compression process from the suction nozzle pressure to the ejector outlet pressure. In the second part, the nominator is defined similarly but considers the expansion process in the motive nozzle.

$$\eta_{EJ} = \chi \cdot \frac{h|_{s=SN,in\ p=p_{out}} - h_{SN,in}}{h_{MN,in} - h|_{s=MN,in\ p=p_{out}}} \tag{8}$$

where h is the specific enthalpy, subscript s refers to the specific entropy in the suction nozzle (*SN*) and the motive nozzle (*MN*), respectively, p refers to the pressure at the ejector inlets (*in*) and outlet (*out*), respectively. In this definition, parameter χ, called the mass entrainment ratio (MER), is defined as the ratio between the suction and the motive mass flow rates.

$$\chi = \frac{\dot{m}_{SN}}{\dot{m}_{MN}} \tag{9}$$

where $\dot{m}$ is the mass flow rate.

4. Results and discussion

4.1. Operating condition influence

Global results of the performed simulations for all three OCs are presented in Fig. 5. Vertical axis of the graph demonstrates the value of the relative increment in MER (ΔMER) defined as:

$$\Delta MER = \frac{\chi_{bypass} - \chi_{baseline}}{\chi_{baseline}} \cdot 100\% \tag{10}$$

The horizontal axis represents values of the bypass position defined by Eq. (1) and displayed in Table 1. The baseline ejector efficiency was found to be 22.2%, 32.6% and 35.2% for OC #1, OC #2 and OC #3, respectively, while the values of the corresponding baseline ejector MER were 0.504, 0.425 and 0.303. Hence, three pairs of point results according to the operating condition number and bypass angle β (19° and 38°) are presented, using crosses and circles, respectively. Moreover, the black colour indicates OC #1, the blue colour is for OC #2 and the red colour is related to OC #3.

The relationship between the ΔMER and the bypass position gives clear information about the prospective operating conditions for this ejector type. Namely, significant increment is visible practically only at OC #1, characterised by the lowest pressure lift of 4 bar. Position 1.4 resulted in the highest MER increment. Namely, the values of 36.9% and 32.0% for the bypass angle 19° and 38°, respectively, have been found. Taking the literature review into account, this improvement could be characterised as high as it indicates potential for further analysis of the bypass idea using an experimental approach.

Almost the same ΔMER was obtained for both angles for Position 1.0 and OC #1. In the case of OCs #2 and #3, the flow resulted in the lowered MER and finally the suction flow was chocked in the ejector mixer. Nevertheless, in the case of the intermediate pressure lift (OC #2), decrement of the suction phenomena was very small (less than 5%) until Position 1.3, possibly suggesting quite a large insensitivity of the mixer ending geometry when transonic carbon dioxide flow is blocked. Moreover, for Position 1.0 of angle 19°, an increment of 1.5% was obtained. Simulations of the lift (OC #3) with the highest pressure of 9 bar resulted in rapid decrement of the MER value, starting immediately from the first bypass position. Introduction of the bypass duct under these conditions deteriorated the suction phenomena in the suction

This is a post-print version of an article published in International Journal of Refrigeration
DOI: 10.1016/j.ijrefrig.2018.03.020

nozzle and pre-mixing chamber. Additionally, there were no favourable pressure conditions in the bypass mixer chamber, so suction flow was also not available in this duct.

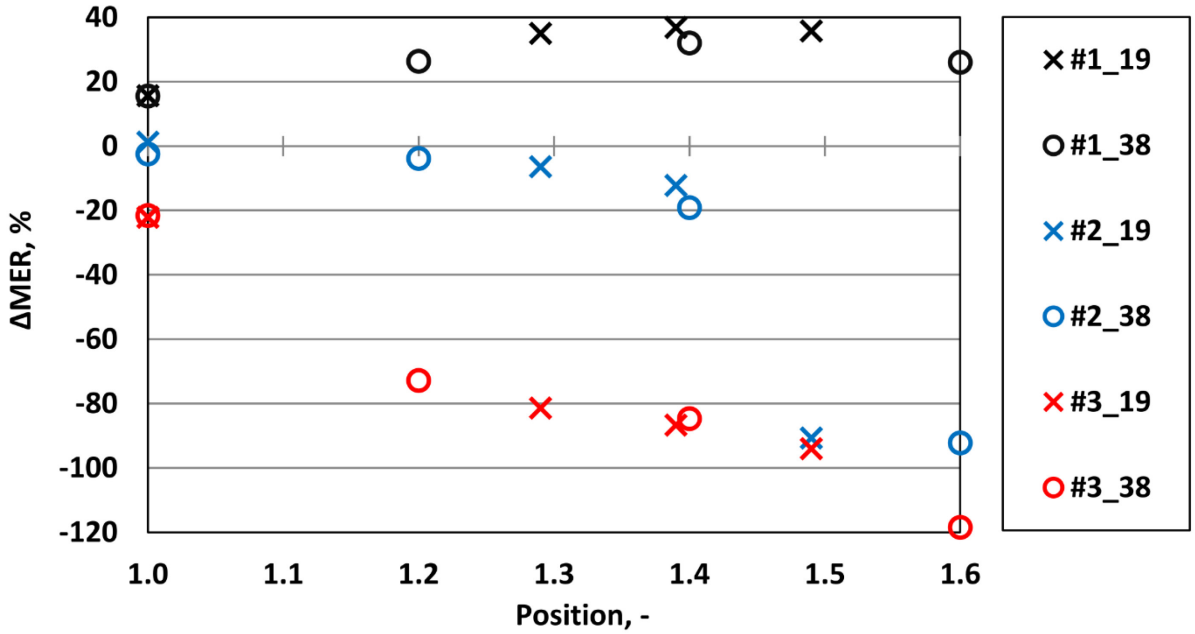

Figure 5. Global results of three operating conditions and various bypass positions.

4.2. Performance results and improvement discussion of OC #1

The detailed results from simulations of OC #1 are presented in Table 3, since these conditions resulted in the most perspective operation of the ejector equipped with the bypass. Namely, every examined bypass position resulted in a significant increment of the ΔMER value. The observed phenomenon of the MER increment is based on the increment of the suction stream with the constant motive stream. In comparison to the baseline case, the smallest ΔMER that was recorded took a value of 15.5%, which still could be described as substantial. Position 1.4 resulted in the maximum improvement of the sucked stream mass flow rate for both angles. The bypass angle of 38° resulted in the ΔMER of 32.0% and for the angle of 19°, this flow parameter increased by 36.9%. As a result, the ejector efficiency was lifted to the level of 30.4% starting from the baseline value of 22%. Hence, the bypass ejector working at lower pressure conditions was as efficient as a baseline ejector operating in high pressure conditions. Another positive statement is related to the character of the efficiency changes. Namely, a similar level of the efficiency was obtained for a given angle within three positions located in the diffuser. If the bypass duct is located in the diffuser, ejector efficiency is dependent on the bypass shape (the angle), while the influence of its precise position becomes less important. Moreover, this also means that the regulation area for the proper angle used is not affected by rapid changes in the ejector performance.

This is a post-print version of an article published in International Journal of Refrigeration
DOI: 10.1016/j.ijrefrig.2018.03.020

Table 3. Results of the simulation based on OC#1.

Angle	Position	Motive port	Suction port	MER	Efficiency	ΔMER
-	-	kg/s	kg/s	-	%	%
Baseline		0.074	0.037	0.504	22.2	-
38°	1	0.074	0.0431	0.582	25.7	15.5
	1.2	0.074	0.0472	0.637	28.1	26.3
	1.4	0.074	0.0493	0.665	29.3	32.0
	1.6	0.074	0.0470	0.635	28.0	26.0
19°	1.0	0.074	0.0432	0.583	25.7	15.6
	1.3	0.074	0.0504	0.680	30.0	35.0
	1.4	0.074	0.0511	0.690	30.4	36.9
	1.5	0.074	0.0507	0.684	30.2	35.8

An analysis of the suction stream distribution is presented in Fig. 6, where the flows through the suction nozzle and the bypass are separately given. The sum of these streams is equal to the value from Table 3, i.e., the mass flow rate of the suction port. Moreover, black symbols present the total stream depending on the bypass position, blue symbols present the suction nozzle stream and red symbols indicate the bypass stream. Similar to Fig. 5, the crosses and circles are used for the bypass angle of 19° and 38°, respectively. The mass flow rate in the suction nozzle in the baseline case was represented by the green dashed line. Finally, the function of the bypass can easily be found out according to clearly distinguished entrained mass flow rate through the suction nozzle and the bypass duct.

According to the total stream results, the optimum bypass position in the case of the angle 19° is barely visible due to the small incremental differences between Positions 1.3, 1.4 and 1.5. A wide range of similar high improvement values allows for higher tolerance in the manufacturing and regulation process. In the case of the angle of 38°, a character of the total stream changes is different and has a visible maximum. The suction nozzle mass flow rate changes are almost linear for both angles, while the values related to the smaller angle are slightly smaller than those for the angle of 38°. Moreover, these streams are growing constantly through the whole range examined. Hence, the maximum points are located at the highest bypass positions. However, the mass flow rate of the suction nozzle is lower than the baseline case for each of the simulated bypasses. In the case of Position 1.5 – after the position of the maximum total stream - this value approaches the baseline. Nevertheless, a character of the bypass results differs between the angles. Moreover, it is not uniform like the changes obtained for the mass flow rate through the suction nozzle. The character of these changes was a source of the same trend of the total stream. The maximum bypass stream is related to Position 1.2 for the angle of 38° and 1.3 for the angle of 19°, which is before the maximum of the total stream. Due to the uniform growth of the flow through the suction nozzle, the highest value of the total stream is slightly farther. Finally, a small difference between the examined angles is visible. Namely, in the case of the smaller angle, the suction stream is higher by almost 8% based on the maximum values. The performance of the suction nozzle is not significantly affected by introducing the considered bypass, and a similar growth is reported in both analysed angles, leading to a

This is a post-print version of an article published in International Journal of Refrigeration
DOI: 10.1016/j.ijrefrig.2018.03.020

statement that the re-design process of the suction nozzle is not necessary in the case of the bypass ejector type.

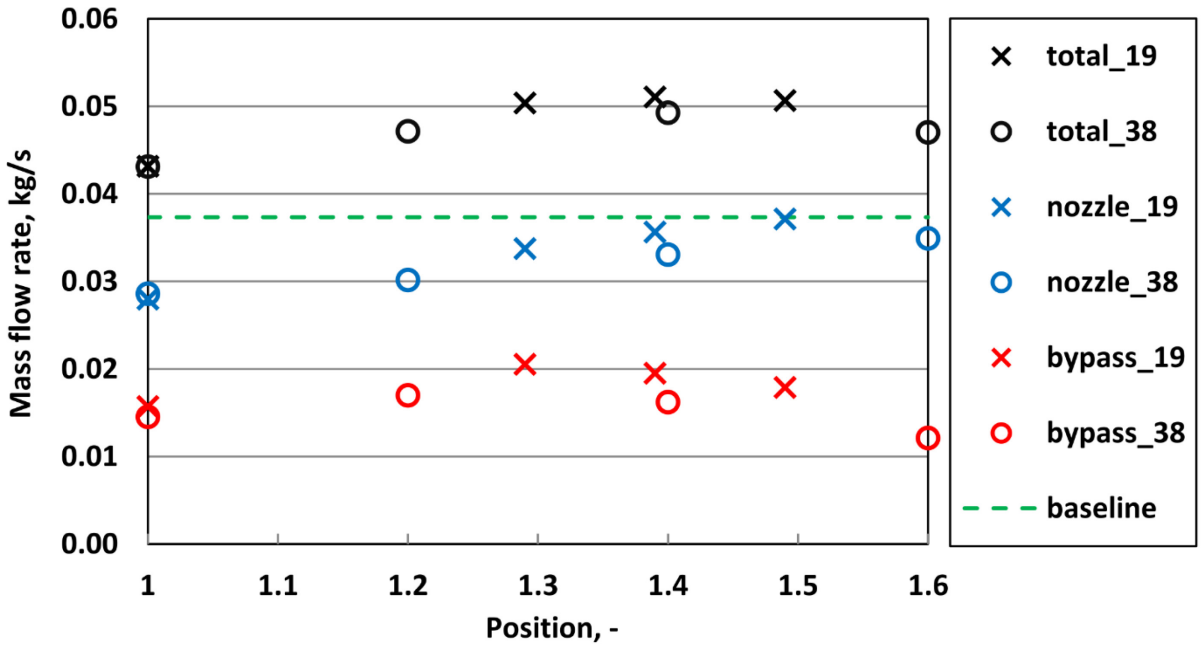

Figure 6. Distribution of total suction mass flow rate for suction nozzle and bypass.

4.3. Field analysis for the bypass configuration with the highest improvement

The highest ΔMER of 36.9% was obtained for the OC #1 mentioned with the smaller angle 19° in Position 1.4. The detailed analysis of the most perspective bypass ejector is presented in the following subsections. First, the pressure distribution along the ejector axis is presented in Fig. 7 using the solid red line for the mentioned case and the dashed black line for the baseline case. The ejector length was presented in the relative form, where 0.0 is the motive nozzle inlet and 1.0 is the ejector outlet. Taking into consideration the distance related to the mixer, the red solid line is located higher than the line related to the baseline ejector. This situation could be related to the lower mass flow rate delivered to the mixing zone through the suction nozzle, as it was presented in Fig. 6. In this zone, the lower mass flow rate resulted in a higher pressure and more intensive mixing process. In the dashed green frame, the detailed view of the diffuser beginning is given. The vertical green line denotes the mixer-diffuser connection, and the vertical red lines indicate the bypass position. The higher pressure previously mentioned in the mixer region (red solid line is above black dashed line) is clearly visible. The absolute pressure at the outlet from mixer in the best bypass case was of approximately 2.50 MPa, while in the baseline case, this parameter is lower, showing 2.03 MPa. The pressure distribution after the bypass suction chamber is more linear than in the baseline case. Additionally, the bypass pressure distribution has a lower average pressure right after the bypass position, corresponding to the phenomenon of the additional mass suction. Finally, after some diffuser length, the pressure distribution along the axis is equal again for both cases discussed.

This is a post-print version of an article published in International Journal of Refrigeration
DOI: 10.1016/j.ijrefrig.2018.03.020

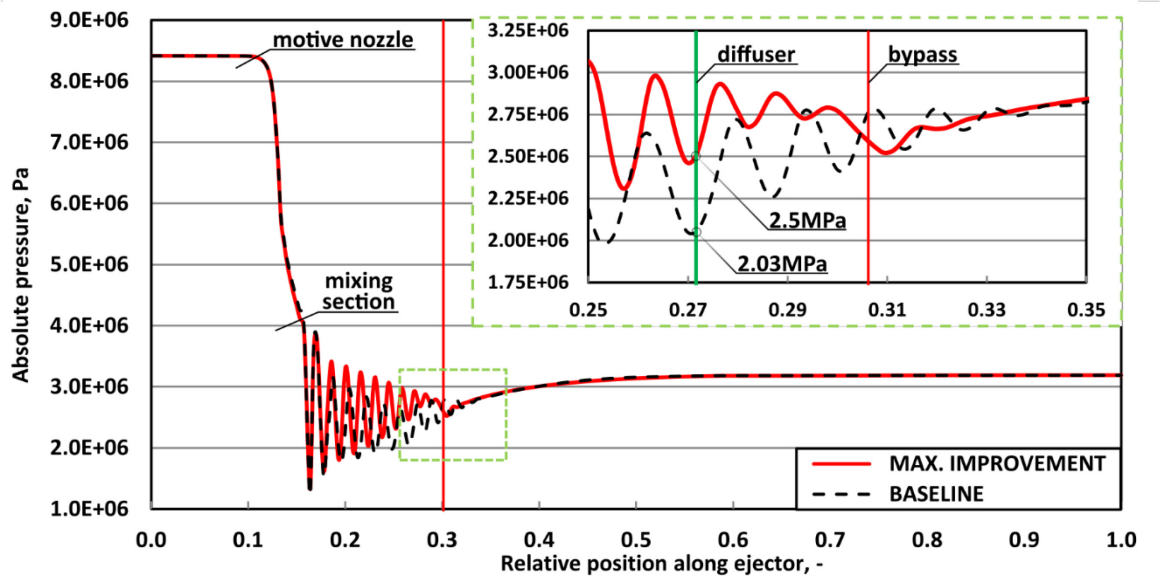

Figure 7. Absolute pressure distribution (Pa) along the ejector axis for the baseline (dashed black) and the best bypass case (red).

An extension of the pressure distribution analysis is continued referring to Fig. 8. In this figure, the absolute pressure field in the whole baseline and bypass ejectors (left) and in the area (dotted red frame) of the bypass suction chamber (right) is presented. Both fields in Fig. 8 contain two symmetrical halves where the left one was obtained from the baseline unit, and the right one was obtained from the bypass ejector simulations.

The absolute pressure field analysis shows some fundamental phenomena. Starting from the motive nozzle, 8.5 MPa pressure is converted to high speed flow. The difference between the baseline and the bypass ejector can be observed in the characteristic shock trains located in both mixing sections. Namely, shift of pressure patterns between analysed cases is clearly visible.

As it was mentioned, the area of the bypass suction chamber was presented in the different pressure range on the right-hand side of Fig. 7 for a better illustration. In addition to the shock train shift, the pressure values in the mixing section are higher for the bypass case than for the baseline case, not only in the ejector axis but also in the wall vicinity. The mixing area of the bypass ejector (right) indicates 2.7 MPa, while the baseline (left) ejector mixer is described by approximately 2.2 MPa, resulting in a difference of approximately 0.5 MPa. Analysis ensured based on the absolute pressure distribution along the ejector axis (previous paragraph) resulted in the similar difference of approximately 0.47 MPa. However, pressure values were slightly lower due to the shock train pattern in the ejector core. These increments could be related to the lower mass flow rate in the mixer, as it was stated on the basis of the mass flow rate distribution presented in Fig. 6.

The pressure field in the cross-section of the bypass suction chamber is uniform on the level of approximately 2.8 MPa. According to the pressure distribution presented in Fig. 7, where the almost linear pressure drop along the suction chamber was presented, a similar pressure distribution is observed for the whole bypass suction chamber. Hence, such a uniform distribution confirmed preliminary assumptions of the bypass width equal to approximately half of the mixer diameter.

Right after the bypass suction chamber, the pressure level is lowered again to approximately 2.5 MPa in the whole diffuser cross-section related to the additional mass flow introduced to the diffuser volume through the bypass. To avoid this additional pressure drop, adjustment of the bypass width or the diffuser width starting from the end of the bypass suction chamber could bring additional improvements. Nevertheless, the bypass width of the mixer half diameter is found to be quite a good choice for the preliminary analysis of the bypass solution.

This is a post-print version of an article published in International Journal of Refrigeration
DOI: 10.1016/j.ijrefrig.2018.03.020

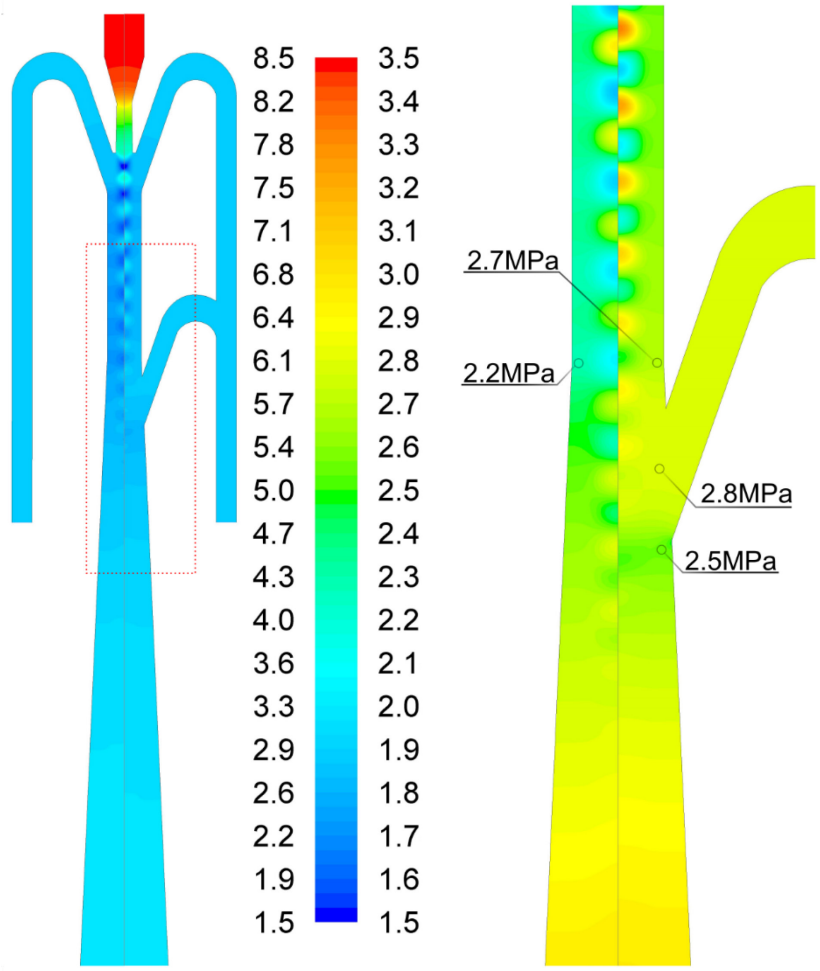

Figure 8. Absolute pressure field (MPa) of the baseline (left) and the bypass ejector (right) in the whole and zoomed views.

The Mach number field is presented in Fig. 9 in the same views as in the previous figures. The distribution of this parameter is mostly a mirror of the pressure distribution. However, some additional comments can be made. First, a supersonic flow was observed right after the motive nozzle throat reaching a Mach number of 1.8 in the pre-mixing chamber. For both cases considered, the baseline and the bypass ejectors, the transcritical state of the fluid is present in the whole mixer, as well as at the beginning of the diffuser. After the bypass implementation, the transcritical area in the mixer was not changed and was approximately more than half of the mixer volume. However, the train shock pattern is slightly silenced before the bypass suction chamber. However, in the bypass ejector case, the Mach number field in further diffuser areas showed higher values than the values for the baseline case, which is again the result of the additional fluid flow and increased velocity of the stream. The diffuser shape optimisation should lead to a more uniform velocity distribution.

This is a post-print version of an article published in International Journal of Refrigeration
DOI: 10.1016/j.ijrefrig.2018.03.020

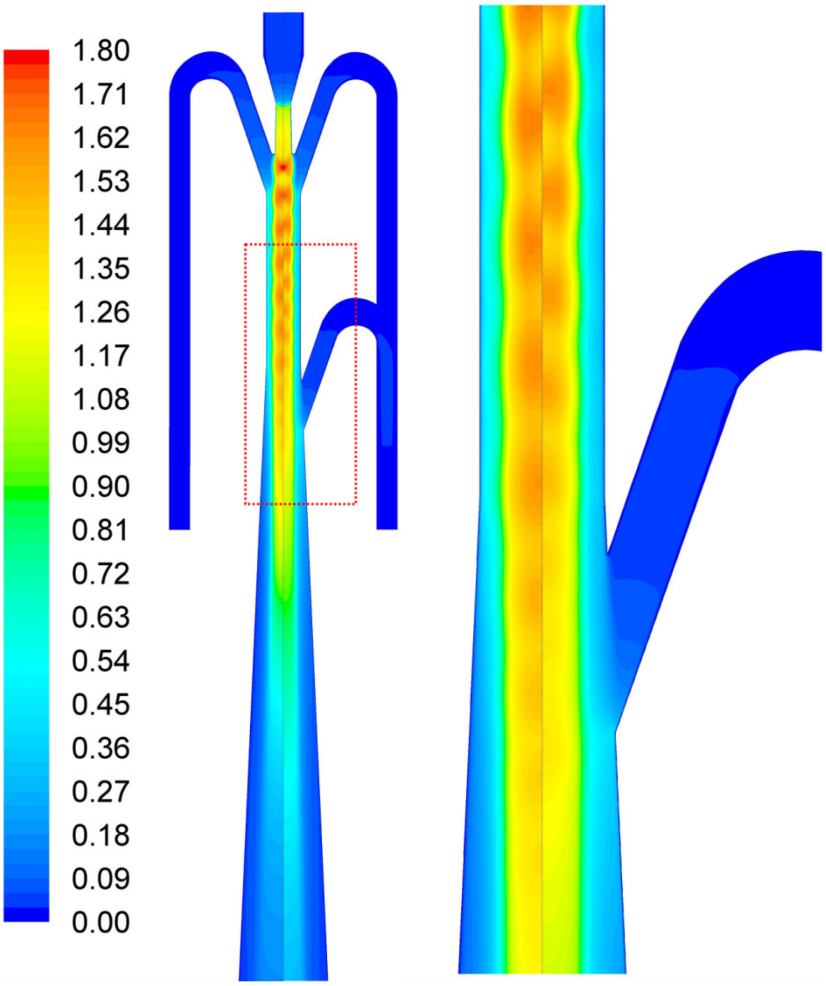

Figure 9. Mach number field of the baseline (left) and the bypass ejector (right) in the whole and zoomed views.

An analysis of the fundamental differences between the best case of the simulated bypass configurations and the baseline case was discussed in the previous subsections. Nevertheless, for the angle of 19° and the bypass Positions 1.3 and 1.5, the results showed a very similar MER increment as it was obtained for the best case (Position 1.4). An attempt was made to capture possible differences. The pressure distribution along the ejector axis for those cases was presented in Fig. 10 in the form of three curves for Positions 1.3 (dashed blue), 1.4 (solid red) and 1.5 (dashed green). Moreover, a vertical line marked the position of each bypass in the corresponding colour. According to the aforementioned small differences of the efficiency improvement, the differences between the pressure distributions of each case are also not large. The character of the pressure distribution right after each bypass position is similar. After the pressure drop related to the additional suction mass flow, an increase of the static pressure is observed due to the flow through the diffuser. However, some substantial features can be noticed in the bypass suction chamber areas, namely, in Positions 1.3 and 1.5, where the pressure fluctuations diminished in the region of the bypass suction chamber. These regions are numbered 1 and 2 in Fig. 10. The length of each flattening is almost the same due to the same length of the bypass suction chamber. However, the length is not exactly the same due to the changing diameter of the diffuser along the bypass positions. In contrast to 1.3 and 1.5, the 1.4 curve has a constant pressure drop along the bypass suction chamber area.

This is a post-print version of an article published in International Journal of Refrigeration
DOI: 10.1016/j.ijrefrig.2018.03.020

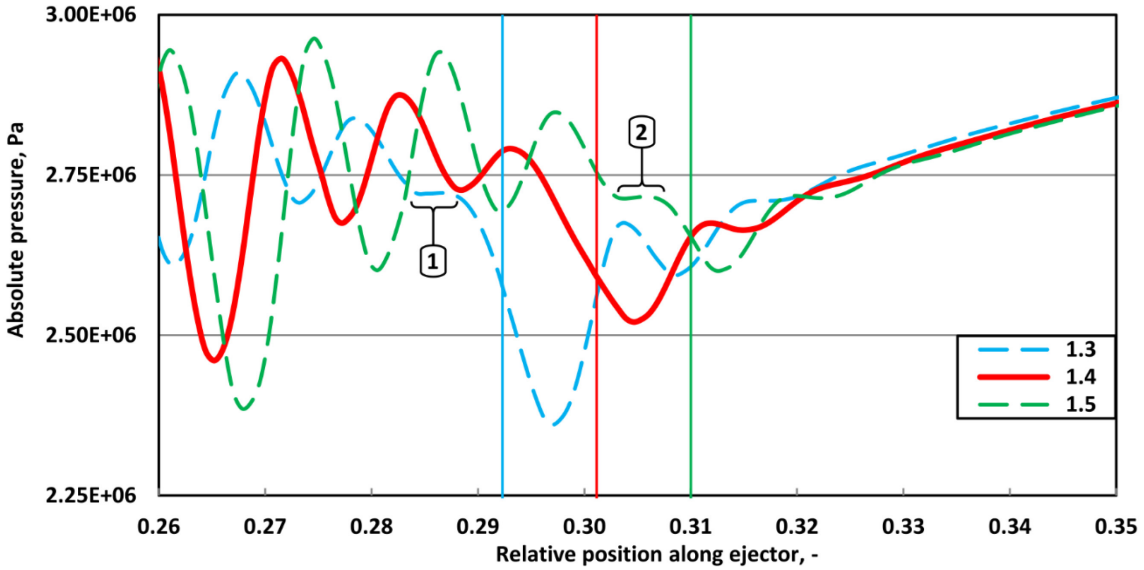

Figure 10. Absolute pressure distribution (Pa) along the axis of ejectors with the bypass angle of 19° for position 1.3 (dashed blue), 1.4 (solid red) and 1.5 (dashed green).

5. Conclusions and further work

The idea of a bypass implementation to the transcritical carbon dioxide ejector was proposed. A control approach of the bypass was also proposed. The bypass idea presented was preliminarily numerically examined based on the operating conditions characterised by high accuracy for the HEM approach employed. The numerical simulations were executed using the well-validated computational platform *ejectorPL*. For the operating conditions with the pressure lift of 4 bar, very promising results were obtained. The ΔMER was 32.0% for the bypass angle 38° and 36.9% for the bypass angle 19°. In order to decisively confirm an opportunity for a ground-breaking increase in COP of the refrigeration system, additional efforts for the bypass prototype design and then further experimental analysis of this solution should be made. The results potential could be evaluated as high enough for such research. The higher pressure lift case did not result in any improvement to the ejector performance.

The translation of the shock train along the ejector axis, as well as the higher pressure in the ejector mixer, was reported because of the bypass implementation. According to the pressure field distribution in the bypass suction chamber, the assumption of the bypass width of a half of the mixer diameter was evaluated as sufficient in the preliminary analysis. Moreover, in the bypass suction chamber, the uniform pressure distribution in the duct cross-section, as well as the constant linear pressure drop, was one of the features characteristic of the highest improvement of the ejector operation.

In the simulation of OC#1 (the lowest pressure lift), small differences between the MER improvements were obtained for the optimum position and the two neighbouring positions considered. We could conclude that very high accuracy of the bypass positioning might be avoided in the operation with the low pressure lift. In such an operation, the bypass angle becomes a more significant factor, leading to the statement that optimisation of the bypass duct profile should bring more benefits than the detailed analysis of the bypass positioning. Finally, from the point of view of ΔMER, the most crucial parameter is the pressure lift of the operation, and then the bypass shape. Finally, based on the first results presented, the bypass position should be located approximately 40% of the mixer length after the diffuser beginning, regarding a properly designed fixed geometry ejector.

Acknowledgements

This is a post-print version of an article published in International Journal of Refrigeration
DOI: 10.1016/j.ijrefrig.2018.03.020

Scientific work was financed from the budget for science in the years 2017-2021, as a research project 08/060/DG_17/0140 under the programme "Diamond Grant". The work of JS, MP and MH was partially supported by the SUT Rector's research grant 08/060/RGP17/0135, 08/060/RGJ17/0108 and 08/060/RGJ18/0157, respectively as well as statutory research fund of the Faculty of Power and Environmental Engineering, Silesian University of Technology.

References

American Society of Heating Refrigerating and Air-Conditioning Engineers. (2016). *ANSI/ASHRAE Standard 34, Designation and Safety Classification of Refrigerants*. Atlanta, GA, USA: ASHRAE.

Anderson, J. D. (1995). *Computational fluid dynamics. The basics with applications.* New York: McGraw-Hill.

Banasiak, K., Hafner, A., Kriezi, E. E., Madsen, K. B., Birkelund, M., Fredslund, K., & Olsson, R. (2015). Development and performance mapping of a multi-ejector expansion work recovery pack for R744 vapour compression units. *Int. J. Refrigeration*, *57*, 265–276. https://doi.org/10.1016/j.ijrefrig.2015.05.016

Banasiak, K., Palacz, M., Hafner, A., Bulinski, Z., Smolka, J., Nowak, A. J., & Fic, A. (2014). A CFD-based investigation of the energy performance of two-phase R744 ejectors to recover the expansion work in refrigeration systems: An irreversibility analysis. *Int. J. Refrigeration*, *40*, 328–337. https://doi.org/10.1016/j.ijrefrig.2013.12.002

Bodys, J., Palacz, M., Haida, M., Smolka, J., Nowak, A. J., Banasiak, K., & Hafner, A. (2017). Full-scale multi-ejector module for a carbon dioxide supermarket refrigeration system: Numerical study of performance evaluation. *Energy Convers. Manag.*, *138*, 312–326. https://doi.org/10.1016/j.enconman.2017.02.007

Bodys, J., Smolka, J., Palacz, M., Haida, M., Banasiak, K., Nowak, A. J., & Hafner, A. (2016). Performance of fixed geometry ejectors with a swirl motion installed in a multi-ejector module of a CO2 refrigeration system. *Energy*, *117*, 1–12. https://doi.org/10.1016/j.energy.2016.07.037

Byrne, P., Miriel, J., & Lenat, Y. (2009). Design and simulation of a heat pump for simultaneous heating and cooling using HFC or CO2 as a working fluid. *Int. J. Refrigeration*, *32*(7), 1711–1723. https://doi.org/10.1016/j.ijrefrig.2009.05.008

Chen, W., Chen, H., Shi, C., Xue, K., Chong, D. T., & Yan, J. (2016a). Impact of operational and geometrical factors on ejector performance with a bypass. *Appl. Therm. Eng.*, *99*, 476–484. https://doi.org/10.1016/j.applthermaleng.2016.01.074

Chen, W., Chen, H., Shi, C., Xue, K., Chong, D., & Yan, J. (2016b). A novel ejector with a bypass to enhance the performance. *Appl. Therm. Eng.*, *93*, 939–946. https://doi.org/10.1016/j.applthermaleng.2015.10.067

Chung, T. J. (2010). *Computational fluid dynamics.* (2nd ed.). Cambridge: University Press.

Elbel, S., & Hrnjak, P. (2008). Experimental validation of a prototype ejector designed to reduce throttling losses encountered in transcritical R744 system operation. *Int. J. Refrigeration*, *31*(3), 411–422. https://doi.org/10.1016/j.ijrefrig.2007.07.013

Elbel, S., & Lawrence, N. (2016). Review of recent developments in advanced ejector

technology. *Int. J. Refrigeration*, *62*, 1–18. https://doi.org/10.1016/j.ijrefrig.2015.10.031

European Commission. (2006). Directive 2006/40/EC of the European Parliament and of the Council of 17 May 2006 relating to emissions from air-conditioning systems in motor vehicles and amending Council Directive 70/156/EEC. *Official Journal of the European Union*, (161), 12–18. https://doi.org/http://data.europa.eu/eli/dir/2006/40/oj

European Commission. (2014). Regulation (EU) No 517/2014 of the European Parliament and of the Council of 16 April 2014 on fluorinated greenhouse gases and repealing Regulation (EC) No 842/2006 Text with EEA relevance. *Official Journal of the European Union*, *57*, 195–230. https://doi.org/doi:10.3000/19770677.L_2013.124.eng

Farsi, A., Mohammadi, S. M. H., & Ameri, M. (2016). An efficient combination of transcritical CO 2 refrigeration and multi- effect desalination : Energy and economic analysis. *Energy Convers. Manag.*, *127*, 561–575. https://doi.org/10.1016/j.enconman.2016.09.038

Ge, Y. T., & Tassou, S. A. (2014). Control optimizations for heat recovery from CO2 refrigeration systems in supermarket. *Energy Convers. Manag.*, *78*, 245–252. https://doi.org/10.1016/j.enconman.2013.10.071

Ge, Y. T., Tassou, S. A., Santosa, I. D., & Tsamos, K. (2015). Design optimisation of CO2 gas cooler/condenser in a refrigeration system. *Appl. Energy*, *160*, 973–981. https://doi.org/10.1016/j.egypro.2014.11.1191

Hafner, A. (2016). R744 train HVAC unit. In *12th IIR Gustav Lorentzen Conference* (p. Paper ID: 1132). Edinburgh, UK.

Hafner, A., Försterling, S., & Banasiak, K. (2014). Multi-ejector concept for R-744 supermarket refrigeration. *Int. J. Refrigeration*, *43*, 1–13. https://doi.org/10.1016/j.ijrefrig.2013.10.015

Haida, M., Banasiak, K., Smolka, J., Hafner, A., & Eikevik, T. M. (2016a). Experimental analysis of the R744 vapour compression rack equipped with the multi-ejector expansion work recovery module. *Int. J. Refrigeration*, *64*(August), 93–107. https://doi.org/10.1016/j.ijrefrig.2016.01.017

Haida, M., Smolka, J., Palacz, M., Bodys, J., Nowak, A. J., Bulinski, Z., Hafner, A. (2016b). Numerical investigation of an r744 liquid ejector for supermarket refrigeration systems. *Therm. Sci.*, *20*(4), 1259–1269. https://doi.org/10.2298/TSCI151210112H

Hurley, M. D., Wallington, T. J., Javadi, M. S., & Nielsen, O. J. (2008). Atmospheric chemistry of CF3CF{double bond, long}CH2: Products and mechanisms of Cl atom and OH radical initiated oxidation. *Chem. Phys. Lett.*, *450*(4–6), 263–267. https://doi.org/10.1016/j.cplett.2007.11.051

Ignacio, J., Villarino, A., & Ángel, F. (2017). Experimental and modelling analysis of an office building HVAC system based in a ground-coupled heat pump and radiant floor. *Appl. Energy*, *190*, 1020–1028. https://doi.org/10.1016/j.apenergy.2016.12.152

Imamura, T., Kamiya, K., & Sugawa, O. (2015). Ignition hazard evaluation on A2L refrigerants in situations of service and maintenance. *J. Loss Prev. Process Ind.*, *36*, 553–561. https://doi.org/10.1016/j.jlp.2014.12.018

IPU & Department of Mechanical Engineering of Technical University of Denmark. (2017). CoolPack; ISO 817:2014; EN 378-1:2008.

Joneydi Shariatzadeh, O., Abolhassani, S. S., Rahmani, M., & Ziaee Nejad, M. (2016). Comparison of transcritical CO2 refrigeration cycle with expander and throttling valve including/excluding internal heat exchanger: Exergy and energy points of view. *Appl. Therm. Eng.*, *93*, 779–787. https://doi.org/10.1016/j.applthermaleng.2015.09.017

Lawrence, N., & Elbel, S. (2015). Mathematical modeling and thermodynamic investigation of the use of two-phase ejectors for work recovery and liquid recirculation in refrigeration cycles. *Int. J. Refrigeration*, *58*, 41–52. https://doi.org/10.1016/j.ijrefrig.2015.06.004

Lemmon, E., Huber, M., & McLinden, M. (2010). *NIST standard reference database 23: reference fluid thermodynamic and transport properties - REFPROP.* (9th ed.). Gaithersburg: National Institute of Standards and Technology, Standard Reference Data Program.

Liu, F., Groll, E. a., & Li, D. (2012a). Investigation on performance of variable geometry ejectors for CO 2 refrigeration cycles. *Energy*, *45*(1), 829–839. https://doi.org/10.1016/j.energy.2012.07.008

Liu, F., Li, Y., & Groll, E. (2012b). Performance enhancement of CO 2 air conditioner with a controllable ejector. *Int. J. Refrigeration*, *35*(6), 1604–1616. https://doi.org/10.1016/j.ijrefrig.2012.05.005

Lorentzen, G. (1994). Revival of carbon dioxide as a refrigerant. *Int. J. Refrigeration*, *17*(5), 292–301. https://doi.org/10.1016/S0016-0032(23)90612-5

Lorentzen, G. (1995). The use of natural refrigerants: a complete solution to the CFC/HCFC predicament. *Int. J. Refrigeration*, *18*(3), 190–197. https://doi.org/10.1016/0140-7007(94)00001-E

Lucas, C., & Koehler, J. (2012). Experimental investigation of the COP improvement of a refrigeration cycle by use of an ejector. *Int. J. Refrigeration*, *35*(6), 1595–1603. https://doi.org/10.1016/j.ijrefrig.2012.05.010

Minetto, S., Cecchinato, L., Brignoli, R., Marinetti, S., & Rossetti, A. (2016). Water-side reversible CO2 heat pump for residential application. *Int. J. Refrigeration*, *63*, 237–250. https://doi.org/10.1016/j.ijrefrig.2015.12.015

Nakagawa, M., Berana, M. S., & Kishine, A. (2009). Supersonic two-phase flow of CO2 through converging-diverging nozzles for the ejector refrigeration cycle. *Int. J. Refrigeration*, *32*(6), 1195–1202. https://doi.org/10.1016/j.ijrefrig.2009.01.015

Nakagawa, M., Marasigan, a. R., Matsukawa, T., & Kurashina, a. (2011). Experimental investigation on the effect of mixing length on the performance of two-phase ejector for CO2 refrigeration cycle with and without heat exchanger. *Int. J. Refrigeration*, *34*(7), 1604–1613. https://doi.org/10.1016/j.ijrefrig.2010.07.021

Nowak, A. J., Palacz, M., Smolka, J., Banasiak, K., Buliński, Z., Fic, A., & Hafner, A. (2015). CFD simulations of transport phenomena during transcritical flow of real fluid (CO2) within ejector. *Int. J. Numer. Methods Heat Fluid Flow*, *26*, 805–817.

Palacz, M., Smolka, J., Fic, A., Bulinski, Z., Nowak, A. J., Banasiak, K., & Hafner, A. (2015). Application range of the HEM approach for CO2 expansion inside two-phase ejectors for supermarket refrigeration systems. *Int. J. Refrigeration*, *59*, 251–258. https://doi.org/10.1016/j.ijrefrig.2015.07.006

Palacz, M., Smolka, J., Nowak, A. J., Banasiak, K., & Hafner, A. (2017). Shape optimisation of a two-phase ejector for CO2 refrigeration systems. *Int. J. Refrigeration*, *74*, 210–221. https://doi.org/10.1016/j.ijrefrig.2016.10.013

Sierra-Pallares, J., García Del Valle, J., García Carrascal, P., & Castro Ruiz, F. (2016). A computational study about the types of entropy generation in three different R134a ejector mixing chambers. *Int. J. Refrigeration*, *63*, 199–213. https://doi.org/10.1016/j.ijrefrig.2015.11.007

Smolka, J., Bulinski, Z., Fic, A., Nowak, A. J., Banasiak, K., & Hafner, A. (2013). A computational model of a transcritical R744 ejector based on a homogeneous real fluid approach. *Appl. Math. Model.*, *37*(3), 1208–1224. https://doi.org/10.1016/j.apm.2012.03.044

Smolka, J., Palacz, M., Bodys, J., Banasiak, K., Fic, A., Bulinski, Z., … Hafner, A. (2016). Performance comparison of fixed- and controllable-geometry ejectors in a CO2 refrigeration system. *Int. J. Refrigeration*, *65*(2011), 172–182. https://doi.org/10.1016/j.ijrefrig.2016.01.025

This is a post-print version of an article published in International Journal of Refrigeration
DOI: 10.1016/j.ijrefrig.2018.03.020